

A HYBRID GP-GWO FRAMEWORK FOR ENHANCED PERFORMANCE OF ROTARY DRYING SYSTEMS

KRUNAL MUDAFLE¹, KANAK KALITA^{1,2,*}, ROBERT CEP², JAN
BLATA³, S.P. SAMAL⁴

¹ Department of Mechanical Engineering, Vel Tech Rangarajan
Dr Sagunthala R&D Institute of Science and Technology,
Avadi, 600062, India. vtd722@veltech.edu.in.
drkanakkalita@veltech.edu.in

² Department of Machining, Assembly and Engineering
Metrology, Faculty of Mechanical Engineering, VSB-
Technical University of Ostrava, 70800 Ostrava, Czech
Republic; robert.cep@vsb.cz

³ Department of Machine and Industrial Design, Faculty of
Mechanical Engineering, VSB-Technical University of
Ostrava, 70800 Ostrava, Czech Republic; jan.blata@vsb.cz

⁴ Department of Biosciences, Saveetha School of Engineering,
Saveetha Institute of Medical and Technical Sciences,
Chennai 602105, India; spsamal24@gmail.com

DOI: 10.17973/MMSJ.2025_03_2025004

drkanakkalita@veltech.edu.in; kanakkalita02@gmail.com

ABSTRACT

This study presents a hybrid framework combining Genetic Programming (GP) and Grey Wolf Optimizer (GWO) to enhance the performance of rotary drying systems. The methodology employs Box Behnken Design (BBD) to investigate the effects of critical process parameters—drying temperature, time, and airflow rate—on moisture ratio (MR). GP is utilized to develop predictive models that capture nonlinear interactions among variables, whereas GWO optimizes the parameters to achieve the desired MR. The proposed GP-GWO framework demonstrates superior predictive accuracy and optimization efficiency compared to traditional methods. It achieves a 1.5% improvement in moisture ratio (MR) optimization over El-Mesery et al.'s model. Experimental validation highlights the framework's ability to minimize moisture ratio while maximizing energy efficiency.

KEYWORDS

Genetic Programming, Grey Wolf Optimizer, Rotary Drying Systems, Process Optimization, Thermal Separation Technology, Desiccant Rotary Dryer

1 INTRODUCTION

Drying is a commonly utilized process in food processing, where it involves thermal removal of moisture content to extend the shelf life of crops and preserve it for long time [Mercer 2023]. Heat transfer to the wet solid can occur through convection, conduction, radiation, or a combination of these mechanisms, facilitating the evaporation of moisture [Jumah 2015]. Dryers are essential devices in process technology used to remove solvents from solid materials. They employ methods such as convective, conductive, or radiative drying to achieve effective thermal separation [Zhou 2021]. Among the various types of dryers, rotary dryers have gained attention for their ability to reduce moisture content in biomass. These devices feature a rotating

drum that ensures uniform drying through controlled airflow and heat application [Daragantina 2020]. Additionally, solar dryers are categorized into direct, indirect, mixed-mode, and hybrid types, each offering different technical performances suitable for various agricultural products [Gautam 2024]. Optimizing the drying process is critical for enhancing shelf life, reducing waste, and improving transportation efficiency of food products. Key process parameters influencing drying efficiency are temperature, humidity, airflow, and drying time. Optimization methods, such as adjusting temperature, feed rate, and drying time, significantly impact the nutritional and sensory quality of dried food products [Homayoonfal 2024].

Bitter melon (*Momordica charantia*), is well known for its nutritional and therapeutic properties. Previous studies have explored various drying techniques for bitter melon. For instance, refractance window drying optimized parameters like temperature, thickness, and blanching time for effective dehydration [Ali 2023]. Ultrasonic-assisted osmotic dehydration followed by hot air-assisted radio frequency drying focused on quality retention and processing efficiency [Guo 2024]. Other methods, such as halogen drying and vacuum drying, investigated the effects of thickness, temperature, and drying conditions on moisture content and chemical quality [Tran 2023]. However, the absence of modelling and optimization in the drying process can lead to inefficient processing, lower yields, increased costs, and suboptimal product quality [Yusuff 2024] [Gao 2024]. Mathematical modelling and optimization enhance drying efficiency by improving moisture evaporation rates and providing a better understanding of drying mechanisms [Rahman 2024]. These approaches lead to superior product quality, reduced drying time, and better retention of nutritional attributes [Borse 2024]. Studies employing Response Surface Methodology (RSM) have demonstrated effective optimization of drying parameters for bitter melon. Models like Page's and Midilli's have shown the best fit for drying kinetics, aiding in optimizing energy consumption and drying processes [Akhoundzadeh Yamchi 2024]. Three-dimensional RSM has also been used to optimize drying conditions, focusing on variables like drying temperature, slice thickness, and blanching time to enhance product quality [Ozsan Kilic 2023]. Despite the widespread use of RSM in modelling and optimizing food drying processes, several factors limit its efficiency. RSM models are typically of a predefined form, often restricted to second-order polynomials [Ali 2023]. This inherent limitation means that the developed models may not capture the complexities of real-life nonlinear data, which may require more complex or more compact equations to accurately represent the system's behavior. In practical scenarios, the relationships between drying parameters and responses can be highly nonlinear and intricate, necessitating more flexible modelling approaches. Additionally, RSM requires supplementary statistical methods like Analysis of Variance (ANOVA) to determine the significance and importance of each parameter in the model [Ali 2023]. This adds an extra layer of complexity to the modelling process and may not efficiently handle the elimination of insignificant terms, potentially leading to less parsimonious models. The reliance on predefined model structures and additional statistical tests can limit the adaptability of RSM in capturing the true dynamics of the drying process.

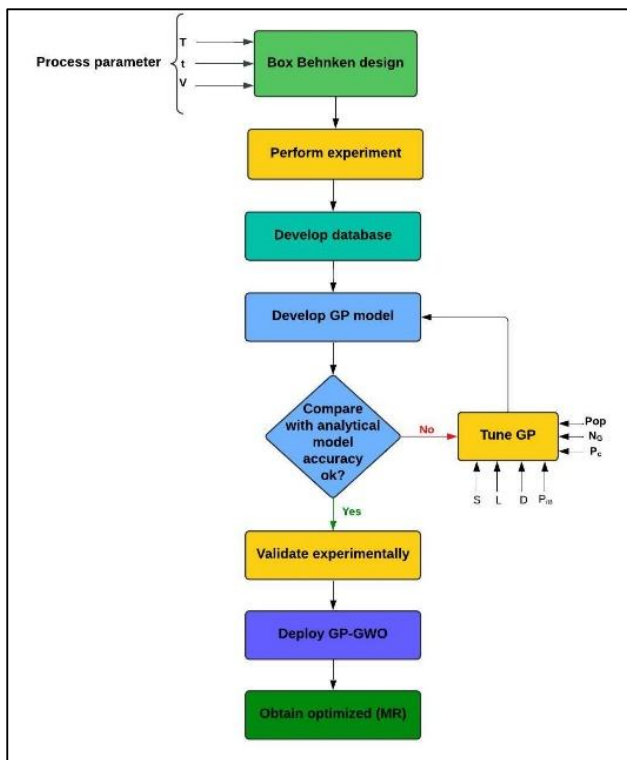


Figure 1. GP-GWO methodology followed in this work

In contrast, Genetic Programming (GP) offers a flexible modelling approach that can inherently handle nonlinearities and complex interactions among variables. GP models evolve over successive iterations, allowing insignificant terms to be eliminated during the training process through built-in mechanisms. This results in models that are potentially more accurate and parsimonious, providing a better fit to the actual data without the need for predefined model structures or additional statistical tests for parameter significance.

Despite these advantages, the application of GP in modelling and optimizing drying processes for agricultural products like bitter melon has not been extensively explored. Previous studies have primarily focused on traditional drying methods and optimization techniques using RSM [Ali 2023] [Ozsan Kilic 2023] [Akhoundzadeh Yamchi 2024], leaving a gap in the literature regarding the use of advanced modelling approaches like GP. Therefore, there is a need to investigate the effectiveness of GP in modelling and optimizing the drying behavior of bitter melon. This approach could potentially overcome the limitations associated with RSM, providing more accurate models that capture the nonlinear dynamics of the drying process. In this paper, by leveraging GP's ability to evolve model structures and eliminate insignificant terms intrinsically, more reliable models are developed. The developed GP model is deployed with GWO to optimize the moisture ratio in drying of bitter melons.

2 METHODOLOGY

The methodology followed in this paper is shown in Figure 1. A Box-Behnken Design (BBD) with three process parameters (temperature (T), drying time (t) and air velocity (V)) is used to perform 15 experiments. The selection of temperature, drying time, and airflow rate as primary process parameters was based on their statistical significance in influencing the drying process. The final significance obtained were temperature = 0.509%, time = 0.345%, and airflow rate = 0.146%. Other potential parameters, such as ambient humidity and initial moisture content, were initially considered but excluded due to their

lower statistical significance in the experimental setup. This decision ensures that the optimization model remains focused on the most impactful variables while maintaining computational efficiency.

A GP model is developed based on this data and after assessing its accuracy it is deployed for process optimization. GWO, a nature-inspired optimization algorithm, is used to ascertain the optimized MR by finding a suitable combination of process parameters. The GP-GWO process begins by using the BBD dataset to create a structured set of input-output relationships using GP. The accuracy of the GP model is verified by comparing its predictions with experimental results. This step ensures that the GP model reliably reflects the process's true behavior. Once validated, the GWO is applied in conjunction with the GP model. GWO uses the GP model's predictions to guide it toward the optimal parameter settings for the system. The final step is to obtain the optimized solution based on the GP-GWO model, which provides the best set of parameters to achieve the desired outcomes. This output represents the optimal configuration for the process, derived from both experimental data and predictive modeling. This methodology integrates experimental design, evolutionary-based predictive modeling and optimization to explore and optimize the drying process. It leverages a minimal number of experimental runs while maximizing insights and delivering optimal solutions through predictive modeling and optimization.

3 EXPERIMENTAL DETAILS

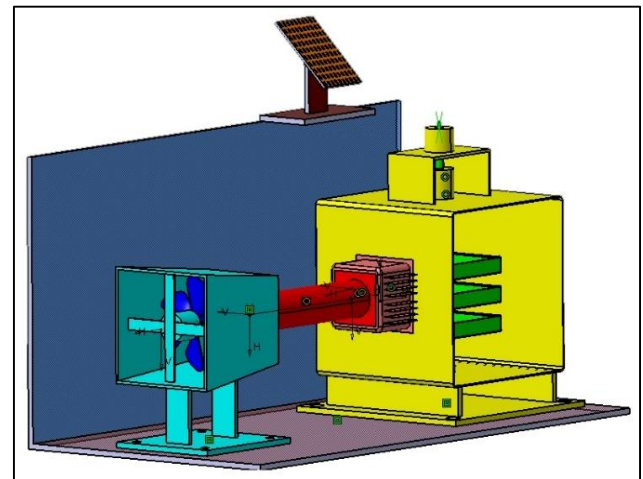


Figure 2. 3D model of the desiccant rotary dryer

Figure 2 shows the 3D model of the indigenously developed desiccant rotary dryer. Figure 3 illustrates the various components of the desiccant rotary dryer. The system starts with ambient air intake. The blower/fan shown on the left side of the model pulls air into the system. The fan controls the airflow direction. Desiccant Drum at the centre houses the desiccant material i.e., silica gel. As the air passes through this rotating drum, the desiccant absorbs moisture from the air, effectively drying it. The rotation allows the desiccant to make full contact with the passing air and provides continuous drying. This system has a solar panel which provides energy to heat the air. The warmer the air entering the desiccant, the more moisture it can absorb, improving the drying process's efficiency. Over time, the desiccant becomes saturated with moisture. The desiccant dryer has a regeneration cycle, where the moisture-laden desiccant is heated, releasing the moisture to be vented out of the system. The solar panel assists with this regeneration process by heating the drum periodically. The temperature (T),

drying time (t) and air velocity (V) are varied for each experiment as per the BBD design.

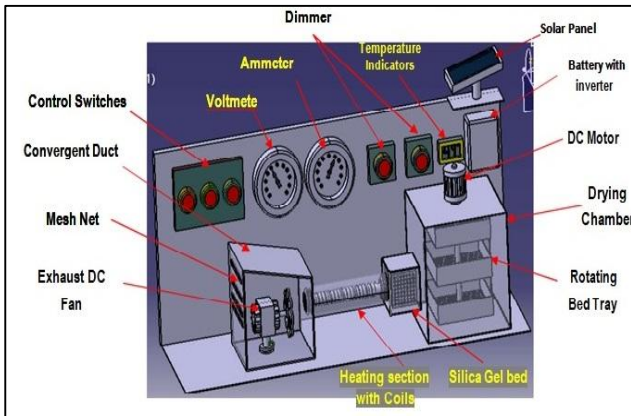


Figure 3. Various components of the desiccant rotary dryer

3.1 Experimentation design with BBD

BBD is employed to optimize the performance of a desiccant rotary dryer. This experimental design methodology allowed for the evaluation of three independent variables— drying temperature (T), drying time (t), and airflow rate (V). The BBD consisted of 15 experimental runs (Table 1), with three levels for each variable. The moisture ratio (MR) of the bitter gourds is measured using,

$$MR = \frac{M_t - M_e}{M_0 - M_e} \quad (1)$$

where M_0 , M_t and M_e are the moisture content at time 0, time t and at equilibrium moisture content respectively. To negate any biases and experimental errors, three independent runs for each experiment are carried out. Further, the experiments are randomized.

3.2 Genetic Programming

GP is an evolutionary algorithm-based approach that generates a predictive model by evolving mathematical expressions or "programs" that best represent the system's behavior. This model can capture complex, nonlinear relationships between inputs and outputs.

3.3 Grey Wolf Optimizer

Grey Wolf Optimizer (GWO) is a nature-inspired optimization algorithm that mimics the leadership hierarchy and hunting mechanism of grey wolves in the wild. In this study, GWO was employed to optimize the drying parameters— T , t and V —to achieve the desired moisture ratio.

The GWO algorithm initializes a population of candidate solutions, each representing a specific combination of drying parameters. These candidates are conceptualized as grey wolves categorized into alpha (α), beta (β), delta (δ), and omega (ω) wolves, based on their fitness levels. The fitness of each candidate solution was evaluated using the GP-derived predictive model for moisture ratio.

During the optimization process, the positions of the wolves are updated iteratively by simulating the social hierarchy and hunting behavior using,

$$\vec{D} = |\vec{C} \cdot \vec{X}_p(t) - \vec{X}(t)| \quad (2)$$

$$\vec{X}(t+1) = \vec{X}_p(t) - \vec{A} \cdot \vec{D}$$

where t indicates the current iteration, $\vec{X}_p(t)$ and $\vec{X}(t)$ represent the position vector of the prey and the grey

wolf at iteration t . \vec{A} and \vec{C} are coefficient vectors, which are calculated as,

$$\vec{A} = 2\vec{a} \cdot \vec{r}_1 - \vec{a} \quad (3)$$

$$\vec{C} = 2 \cdot \vec{r}_2$$

where components of \vec{a} are linearly decreased from 2 to 0 throughout iterations and \vec{r}_1, \vec{r}_2 are random vectors $[0,1]$.

The GWO algorithm converges when the change in the fitness function between iterations falls below a predefined threshold or after a set number of iterations. The optimal drying parameters obtained from GWO were validated experimentally to ensure practical applicability.

4 RESULTS AND DISCUSSION

4.1 Development of GP model

Based on the methodology discussed above, the GP model is developed based on the experimental data shown in Table 1. For training the GP model, various combinations of the turning parameters were considered and the finalized optimal tuning parameters are reported in Table 2. The linearly decreasing value of a from 2 to 0 controls exploration-exploitation trade-off.

During the GP training phase, various characteristics of the GP model are studied and reported in Figure 4. In Figure 4(a) the relative frequency of the terminals and functions across iterations is shown, which depicts how the GP model's building blocks (terminals and functions) evolve over iterations. Terminals represent input variables or constants, while functions represent operations (e.g., +, -, *, /). At the start of the training process, the distribution of terminals and functions is normal and as iterations elapse gradual increase in frequency of significant functions and terminals while decrease in insignificant components is seen. Similarly in Figure 4(b) it is depicted that initially the training process starts with equal weighting of variables which then gradually increases for significant variables. Thus, the insignificant terms would be minimized or eliminated as the GP model evolves over iterations. This shows the contrast of the GP modelling over traditional methods like RSM, where additional tests like ANOVA and stepwise elimination are necessary to identify and eliminate insignificant terms. In Figure 4(c) the convergence of GP is shown which indicates that the GP reaches a high fitness in relatively a smaller number of iterations. The depth and length of the GP tree can have a significant impact on the complexity of the GP model. Thus, for this study the maximum tree length and depth are restricted to 30 and 6 respectively. In Figure 4(d), the maximum, minimum and average depth of the GP trees during stage is monitored. It shows that during each iteration several GP trees are constructed and evaluated whose complexity can be of varying proportions.

Drying Temperature, T ($^{\circ}\text{C}$)	Drying Time, t (min)	Air Flow Rate, V (m/s)	Moisture Ratio, MR	GP (proposed)	[El-Mesery 2023]
50	3000	1	0.323379	0.328908494	0.2857
65	3000	1	0.331648	0.333739618	0.298615
50	4200	1	0.3401	0.336545306	0.2857
65	4200	1	0.333632	0.346645831	0.298615

50	3600	0.5	0.295054	0.299130883	0.255
65	3600	0.5	0.294621	0.303083354	0.267915
50	3600	1.5	0.348033	0.3561584	0.3164
65	3600	1.5	0.370106	0.368015811	0.329315
57.5	3000	0.5	0.304461	0.29841196	0.2614575
57.5	4200	0.5	0.309952	0.303461802	0.2614575
57.5	3000	1.5	0.356106	0.354001631	0.3228575
57.5	4200	1.5	0.373082	0.369151157	0.3228575
57.5	3600	1	0.344403	0.337816938	0.2921575
57.5	3600	1	0.344721	0.337816938	0.2921575
57.5	3600	1	0.343541	0.337816938	0.2921575
57.5	3600	1	0.335683	0.337816938	0.2921575

Table 1. Experimental MR and predictions by proposed GP model and El-Mesery et al.'s model

GP parameter	Value	GWO parameter	Value
Max. Iteration	200	Max. Iteration	100
Population	50	Population	30
Max. tree length	30	α	Linearly decreased from 2 to 0
Max. tree depth	6	-	-
Loss function	MSE	-	-
Crossover probability	90%	-	-
Mutation probability	10%	-	-
Elites per generation	2	-	-

Table 2. Tuning parameters of GP and GWO

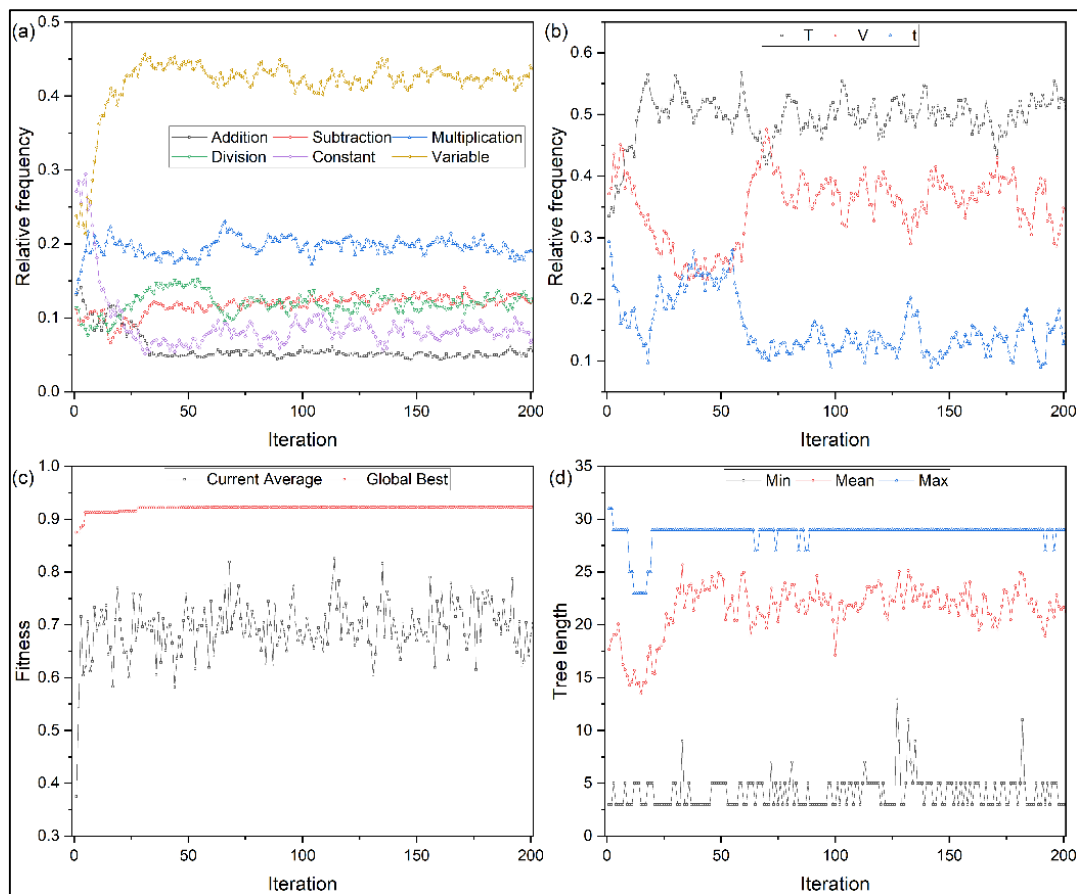


Figure 4. Training progress of the GP models (a) relative frequency of terminals and functions (b) relative frequency of variables (c) fitness of GP model (d) variation on GP tree length across iterations.

Figure 5 shows the proposed GP model in the form of a GP tree. Its length and depth are 20 and 4 respectively. The proposed GP model is mathematically expressed as

$$MR = \left(\beta_0 + \beta_1 \cdot V + \beta_2 \cdot V \cdot T + \frac{\beta_3}{V} + \frac{\beta_4 \cdot V \cdot T}{t} \right) \quad (1)$$

where, $\beta_0 = 0.31637$; $\beta_1 = -0.02115$; $\beta_2 = 0.00155$; $\beta_3 = -0.01715$; $\beta_4 = -0.03207$;

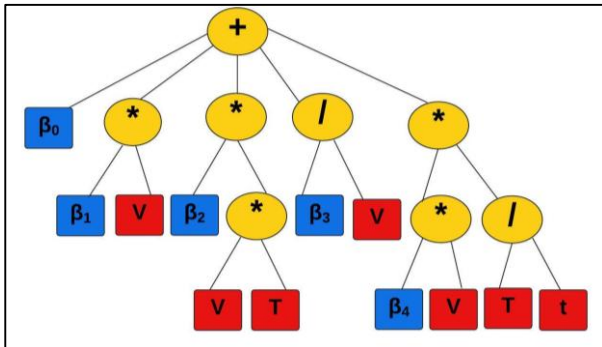


Figure 5. Tree structure of the developed GP model

4.2 Predictive performance of GP model

Figure 6 illustrates the predictive performance of the GP model by studying various aspects of it. Figure 6(a) compares the GP predictions with experimental results. The points aligned closer to the diagonal line indicate a strong agreement between experimental and predicted values. Similarly, Figure 6(b) assesses the residuals against predicted values. The spread of points around zero without any clear pattern implies that the model's prediction errors are randomly distributed. This randomness is desirable, as it suggests that there are no systematic biases in the GP model's predictions. Figure 6(c) is a normal probability plot of the residuals, comparing the distribution of residuals with a normal distribution. Most points fall within the reference line and the upper and lower

percentiles, which indicates that the residuals are approximately normally distributed. This normality of residuals further validates the GP model, as it suggests that the residuals are random and not influenced by unmodeled factors.

Figure 7 shows the variation of the MR with respect to temperature (T), drying time (t), and air velocity (V). It shows that at higher air velocities, MR values are generally higher across the range of temperatures and drying times. This indicates that increased air velocity contributes to a slower drying rate, as the moisture ratio remains higher. The plot also shows that MR decreases with increasing temperature and drying time across all velocities, suggesting that higher temperatures and prolonged drying times enhance the drying process, lowering MR.

To further assess the performance of the GP-GWO model, a comparison was conducted with El-Mesery et al.'s model. While both models demonstrated the ability to optimize moisture ratio (MR), the GP-GWO model consistently provided more accurate predictions, as seen in Figure 8 and Table 3. The proposed GP model aligns closely with the experimental values, with minor deviations across the experiments. In comparison, El-Mesery et al.'s model consistently underestimates MR values. This pattern suggests that while El-Mesery et al.'s model captures some trends, it may not fully capture the complexities of the drying process as effectively as the GP model. Specifically, the GP-GWO model achieved an R^2 of 92.28% and an MSE of 0.0023, whereas El-Mesery et al.'s model exhibited higher deviations from experimental results. The key advantage of the GP-GWO model lies in its ability to capture complex nonlinear relationships without requiring predefined model structures, unlike traditional response surface methods. This enhanced flexibility allows for improved optimization accuracy and robustness in real-world applications.

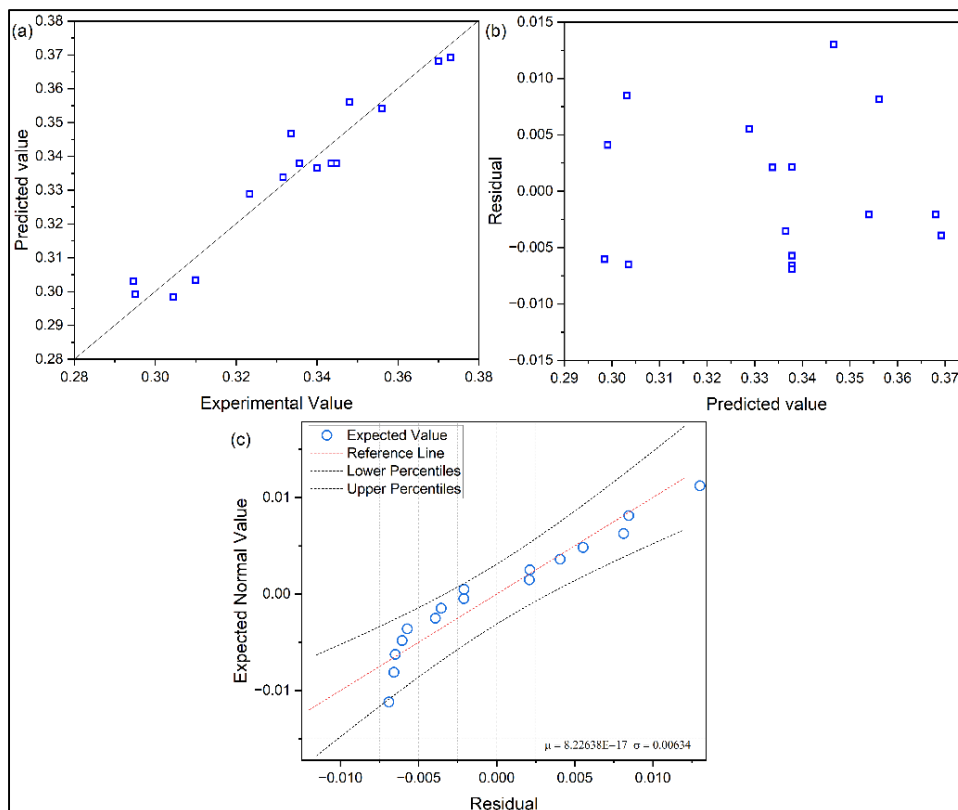


Figure 6. Predictive performance of the GP model (a) experimental versus GP predicted MR (b) GP predicted MR versus its residuals (c) normal probability of residuals.

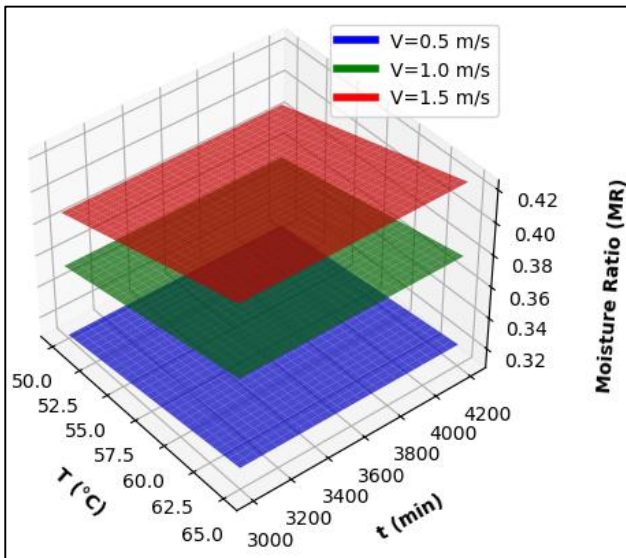


Figure 7. Variation of MR with respect to T and t at various V .

4.3 Optimization using GWO

Figure 9 illustrates the convergence behavior of the Grey Wolf Optimizer (GWO) algorithm over 100 iterations in terms of fitness values. At the initial stages (iterations 0-10), there is a significant drop in both the best and average fitness values, indicating that the algorithm quickly explores and identifies a promising solution region. After this rapid decline, the best fitness curve stabilizes, showing only minor improvements in the remaining iterations, suggesting that the GWO algorithm has found a near-optimal solution and is now refining it through exploration-exploitation balance. The average fitness curve fluctuates slightly throughout, indicating ongoing exploration by the population.

GP-GWO model in optimizing drying conditions. The optimized parameters suggest a moderate temperature, extended drying time, and relatively low air flow rate.

The results demonstrate that the proposed GP-GWO model not only provides more accurate predictions but also achieves better optimization performance compared to El-Mesery et al.'s model. The observed deviations suggest that while El-Mesery et al.'s model captures general drying trends, it fails to fully account for nonlinear parameter interactions, which GP effectively models.

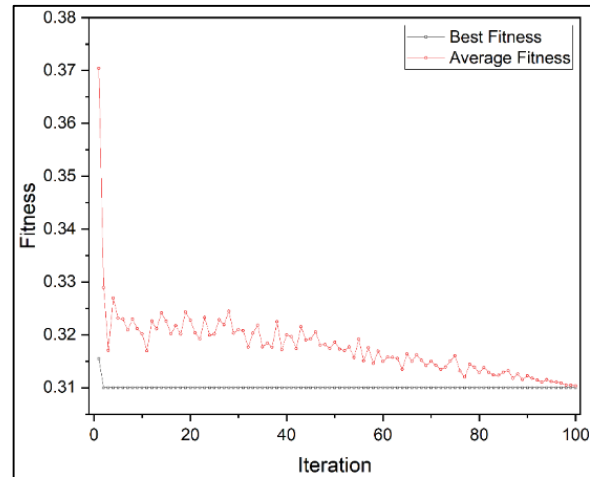


Figure 9. Convergence of the GWO algorithm
Table 3. Optimized parameters predicted by GP-GWO

4.5 Scalability and Industrial Applications

T (°C)	t (min)	V (m/s)	MR	GP	El-Mesery et al.
50	3000	0.5	0.3	0.29	0.2857

The proposed GP-GWO framework, though effective in optimizing drying parameters in laboratory settings, must be evaluated for scalability in industrial-scale systems. Scaling up would require addressing several key challenges like increased computational complexity, real-time adaptability and integration with industrial automation systems. One primary concern is the computational cost of GP models as the dataset size increases. However, this can be mitigated using parallel computing techniques or hybrid models that integrate deep learning for feature extraction. Additionally, industrial drying systems often operate under fluctuating environmental conditions, necessitating adaptive optimization techniques. Future work should explore real-time implementation of the GP-GWO framework using IoT-enabled monitoring systems for enhanced predictive control. Moreover, incorporating additional constraints related to mechanical durability, energy efficiency and maintenance costs will be critical for successful large-scale deployment.

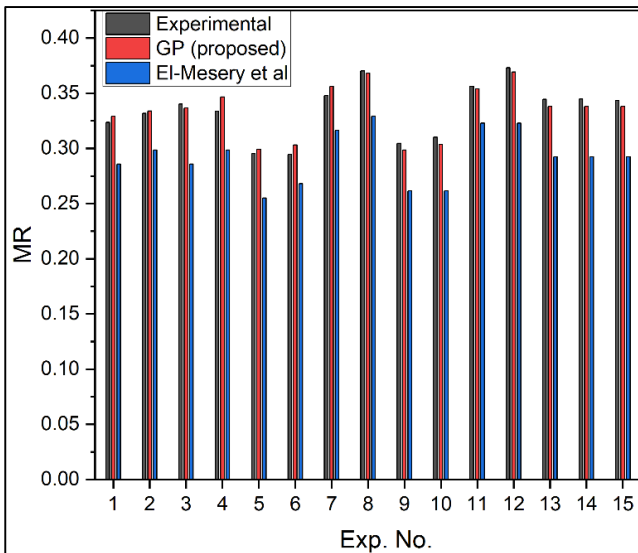


Figure 8. Comparison of the proposed GP model with experimental and El-Mesery et al.'s model

4.4 MR optimization with GP-GWO

Table 3 presents the optimized drying parameters predicted by the hybrid Genetic Programming-Grey Wolf Optimizer (GP-GWO) model. The results show that the GP-GWO model has identified the optimal combination of drying conditions to achieve minimum moisture ratio. Specifically, the optimized parameters are drying temperature of 50°C, drying time of 3000 minutes, air flow rate of 0.5 m/s. Under these conditions, the predicted moisture ratio is 0.29 by GP-GWO model as compared to 0.2857 by El-Mesery et al.'s model (implying a 1.5% difference). These results demonstrate the effectiveness of the

5 CONCLUSION

Based on the comprehensive experiments the following conclusions are drawn—

- The proposed hybrid GP-GWO framework effectively models and optimizes rotary drying systems, addressing nonlinear interactions among process parameters.
- Genetic Programming (GP) demonstrated superior predictive accuracy compared to conventional methods, achieving an R^2 of 92.28% and an MSE of 0.0023. This highlights the robustness of GP in capturing complex nonlinearities more effectively than traditional approaches.

- Grey Wolf Optimizer (GWO) successfully optimized key drying parameters—temperature, time, and airflow rate—to minimize moisture ratio.
- Experimental validation confirmed that the GP-GWO approach outperformed traditional models, such as El-Mesery et al.'s, in both accuracy and optimization efficiency.

Future research directions should focus on enhancing the adaptability of the GP-GWO framework for real-time optimization in industrial environments. One potential avenue is to integrate deep learning models with GP to improve predictive accuracy while reducing computational overhead. Additionally, exploring multi-objective optimization techniques could enable simultaneous optimization of multiple performance metrics, such as energy efficiency and drying uniformity. Another important area of investigation is the incorporation of reinforcement learning to dynamically adjust drying parameters based on real-time feedback from industrial sensors. Expanding the application of GP-GWO to other thermal separation processes, such as freeze-drying and spray drying, could further validate its robustness across diverse industries.

ACKNOWLEDGMENT

This article was co-funded by the European Union under the REFRESH – Research Excellence For REgion Sustainability and High-tech Industries project number CZ.10.03.01/00/22_003/0000048 via the Operational Programme Just Transition and has been done in connection with project Students Grant Competition SP2025/062 „Specific research on progressive and sustainable production technologies“ financed by the Ministry of Education, Youth and Sports and Faculty of Mechanical Engineering VŠB-TUO.

6 REFERENCES

[**Akhoundzadeh Yamchi 2024**] Akhoundzadeh Yamchi, A., Hosainpour, A., Hassanpour, A., & Rezvanivand Fanaei, A. Developing ultrasound-assisted infrared drying technology for bitter melon (*Momordica charantia*). *J. Food Process Eng.*, vol. 47, no. 1, 2024.

[**Ali 2024**] Ali, S., Narwari, I. R., & Faisal, S. Response surface optimization of refractance window drying of bitter gourd slices. *S. J. Agric. Eng. (India)*, vol. 61, no. 1, pp. 52–66, 2024.

[**Borse 2024**] Borse, S. M., Singh, M., Kaur, P., Singh, S., & Zalpouri, R. Drying behavior and nutritional quality of bitter-gourd slices dried in a solar dryer with tray and skewer arrangement. *Environ. Prog. Sustain. Energy*, vol. 43, no. 5, 2024.

[**Daragantina 2020**] Daragantina Nursani, Harry Hafitara, Bariq Bagawanta, & Adi Surjo. Investigation of rotary dryer performance fueled with wood pellets for biomass processing. IOP Conf. Ser.: Earth Environ. Sci., vol. 749, *International Conference of Biomass and Bioenergy*, 10–11 Aug. 2020.

[**Dinh Anh Tuan Tran 2023**] Dinh Anh Tuan Tran, Van Tuan Nguyen, Dinh Nhat Hoai Le, & Thi Khanh Phuong Ho. Study on drying of bitter gourd slices based on halogen dryer. *Res. Agric. Eng.*, vol. 69, no. 3, pp. 143–150, 2023.

[**El-Mesery 2023**] El-Mesery, H. S., Tolba, N. M., & Kamel, R. M. Mathematical modelling and performance analysis of airflow distribution systems inside convection hot-air dryers. *Alexandria Eng. J.*, vol. 62, pp. 237–256, 2023.

[**Gao 2024**] Gao, X., Ma, J., Li, F., Zhou, Q., & Gao, D. Optimization of the extraction process of total steroids from *Phyllinus gilvus* (Schwein.) Pat. by artificial neural network (ANN)-response surface methodology and identification of extract constituents. *Prep. Biochem. Biotechnol.*, pp. 1–14, 2024.

[**Gautam 2024**] Gautam, J. K., & Verma, P. Review paper on different types of solar dryer. *Int. J. Res. Appl. Sci. Eng. Technol.*, vol. 12, no. 7, pp. 250–257, 2024.

[**Guo 2024**] Guo, Q., Zhang, M., Mujumdar, A. S., & Yu, D. Drying technologies of novel food resources for future foods: Progress, challenges and application prospects. *Food Biosci.*, p. 104490, 2024.

[**Homayoonfal 2024**] Homayoonfal, M., Malekjani, N., Baeghbali, V., Ansarifard, E., Hedayati, S., & Jafari, S. M. Optimization of spray drying process parameters for the food bioactive ingredients. *Crit. Rev. Food Sci. Nutr.*, vol. 64, no. 17, pp. 5631–5671, 2024.

[**Jumah 2015**] Jumah, R. Y., & Mujumdar, A. S. Dryer emission control systems. In *Handbook of Industrial Drying*, vol. 2, pp. 1179–1226, 2015.

[**Mercer 2024**] Mercer, D. G. Concepts of dehydration and drying for small-scale food processors. *Royal Society of Chemistry*, ISBN 978-1-83767-367-4, August 2024.

[**Ozsan Kilic 2023**] Ozsan Kilic, T., Boyar, I., Gungor, K. K., Torun, M., Perendeci, N. A., Ertekin, C., & Onus, A. N. Improvement of hot air dried bitter gourd (*Momordica charantia* L.) product quality: Optimization of drying and blanching process by experimental design. *Agriculture*, vol. 13, no. 9, p. 1849, 2023.

[**Rahman 2024**] Rahman, R. A., Sulistyono, S., Utomo, M. S. K. T. S., Gunawan, K. R., & Ismail, I. Investigation on the effect of operation of solar dryer technology according to the drying characteristic of dried product. *Eureka Phys. Eng.*, no. 4, pp. 90–100, 2024.

[**Yusuff 2024**] Yusuff, A. S., & Gu, Y. Studies on effective catalytic conversion of xylose to furfural using green sulfonated carbon catalysts: Process optimization by Taguchi approach. *Arabian J. Chem.*, vol. 17, no. 9, p. 105892, 2024.

[**Zhou 2022**] Zhou, H. Integration and Optimization of Unit Operations. Elsevier, pp. 145–176, 2022.